International Journal of Thermophysics, Vol. 12, No. 1, 1991

Thermal Diffusivity Measurements by Ångström's Method in a Fluid Environment

B. Sundqvist[1]

Received March 12, 1990

Ångström's method has been used for measuring the thermal diffusivity, a, and the radial heat loss coefficients of a thin constantan wire, both in a vacuum and with the wire immersed in air and in four different liquids, and using temperature wave periods of 1 to 1000 s. The presence of a surrounding fluid medium causes errors of up to 90% in the measured values of a. It is shown that both the experimental errors and the radial heat loss coefficients can be accurately calculated using simple models, both at high and at low frequencies, and that a previously developed two-frequency model can be used to obtain accurate data for a even under these conditions, provided the frequency is high enough. We also present a new variety of Ångström's model, valid only at very low frequencies and with purely convective heat loss.

KEY WORDS: Ångström's method; constantan; thermal conductivity; thermal diffusivity.

1. INTRODUCTION

We have previously studied the thermal diffusivity, a, of several metals and alloys under high pressures [1–3] using a modified version [4] of Ångström's classical method [5–7]. To avoid anisotropic strain, such measurements must be performed under hydrostatic conditions in a fluid pressure transmitting medium, in which case convection currents cannot be avoided. A large amount of work has been carried out to find a suitable medium to eliminate this possible source of error. Glycerol, either pure or mixed with glass beads [8], is almost free from convection effects but often crystallizes at about 0.5 GPa (5 kbar), while high-viscosity silicone oils solidify near 1 GPa. A 9:1 glycerol:ethanol mixture does not crystallize but

[1] Department of Experimental Physics, University of Umeå, S-901 87 Umeå, Sweden.

0195-928X/91/0100-0191$06.50/0

is still viscous enough not to allow convection currents and has recently been our preferred medium [3].

We report here a study of the effects of convective radial heat loss on the accuracy of thermal diffusivity measurements by Ångström's method and its many variations. This study was carried out partly to verify that the two-frequency method of Sundqvist and Bäckström [4] works in viscous fluid media and, partly, to try to find a simple criterion for avoiding convection effects. Since the viscosity of all fluids increases with pressure, the study was carried out at atmospheric pressure, which is the worst case situation. We have studied the heat loss from a sample under various circumstances, and we have found an approximate expression for predicting under what conditions the experimental error becomes unacceptably high. We also present a new modification of Ångström's method [Eq. (13) below], valid only under extreme conditions of convective heat loss.

2. THEORY

2.1. Condensed Theory for Ångström's Method and Some of Its Variations

We repeat briefly the theory for Ångström's method [5–7], mainly to define the notation used. In this method, a rod is heated at one end by a periodically varying power. The resulting axial temperature wave is studied at two points along the rod, and a is calculated from the phase shift Φ and the attenuation q of the wave. The temperature along the rod is given by [5–7]

$$a(d^2T/dx^2) = dT/dt + \mu T \tag{1}$$

where μT takes into account radial heat loss. The solution to Eq. (1) is

$$T(x, T) = T_0 \exp[(\alpha + i\beta)x + i\omega t] \tag{2}$$

where $\alpha = (\ln q)/L$, $\beta = \Phi/L$, ω is the angular frequency of the temperature wave, and L is the distance between the two measurement points on the sample. In Ångström's original method [5–7], μ is a real constant and

$$\alpha = [\mu + (\mu^2 + \omega^2)^{1/2}]^{1/2}/(2a)^{1/2} \tag{3a}$$

$$\beta = [-\mu + (\mu^2 + \omega^2)^{1/2}]^{1/2}/(2a)^{1/2} \tag{3b}$$

μ is easily eliminated between Eqs. (3a) and (3b) and a can be obtained as

$$a = \omega/2\alpha\beta = \omega L^2/(2\Phi \ln q) \tag{4}$$

If desired, μ can also be calculated from the measured quantities as

$$\mu = a(\alpha^2 - \beta^2) = (a/L^2)[(\ln q)^2 - \Phi^2] = \omega[(\ln q)^2 - \Phi^2]/(2\Phi \ln q) \tag{5}$$

Contrary to popular opinion [6, 9], a real μ can take into account only heat loss through radiation or forced convection [10], and a rod immersed in a dense medium loses heat mainly by conduction or convection. In the case of pure conduction (solid medium), we can use the theory for radial heat loss from a periodically heated cylindrical rod of radius r [10] to find [4]

$$\mu = \mu_1 + i\mu_2 = (2\lambda_m \eta / r^2 \rho c_p)\, K_1(\eta)/K_0(\eta) \tag{6}$$

where $K_n(\eta)$ are modified Bessel functions [10] of complex arguments $\eta = ri^{1/2}(\omega/a_m)^{1/2}$, λ_m and a_m are the thermal conductivity and the thermal diffusivity of the medium, respectively, and ρ and c_p are the density and the specific heat capacity of the material studied. Replacing μ in Eq. (1) by $\mu_1 + i\mu_2$ and solving as before, we find

$$\alpha = \{\mu_1 + [\mu_1^2 + (\omega + \mu_2)^2]^{1/2}\}^{1/2}/(2a)^{1/2} \tag{7a}$$

$$\beta = \{-\mu_1 + [\mu_1^2 + (\omega + \mu_2)^2]^{1/2}\}^{1/2}/(2a)^{1/2} \tag{7b}$$

Ångström's original method is no longer valid, since $\alpha\beta = (\omega + \mu_2)/2a$, or

$$a = (\omega + \mu_2)/2\alpha\beta = (\omega + \mu_2)\, L^2/(2\Phi \ln q) \tag{8}$$

but a can still be found by repeating the measurements at two different frequencies ω_j $(j = 1, 2)$ [4]. Defining

$$Q_1(\eta) = \mu_1(\omega_1)/\mu_1(\omega_2) = [\alpha(\omega_1)^2 - \beta(\omega_1)^2]/[\alpha(\omega_2)^2 - \beta(\omega_2)^2] \tag{9a}$$

$$Q_2(\eta) = \mu_2(\omega_1)/\mu_2(\omega_2) \tag{9b}$$

we can calculate $Q_1(\eta)$ and $Q_2(\eta)$ from Eq. (6) for any given ratio ω_1/ω_2 and, thus, find numerically a function $Q_2 = Q_2(Q_1)$. By measuring q_j and Φ_j at the frequencies ω_j we can calculate Q_1 from Eq. (9a); from this we easily find Q_2 using the known function $Q_2(Q_1)$, and a is then calculated from [4]

$$a = (\omega_2 Q_2 - \omega_1)/[2(\alpha_2\beta_2 Q_2 - \alpha_1\beta_1)] \tag{10}$$

Subscript j denotes value measured at ω_j; as before, $\alpha_j = (\ln q_j)/L$ and $\beta_j = \Phi_j/L$. Equation (10) has been used in a number of high pressure studies of a [1–3]. As before, the heat loss coefficients are easily found from Eq. (7):

$$\mu_1 = a(\alpha^2 - \beta^2) = (a/L^2)[(\ln q)^2 - \Phi^2] \tag{11a}$$

$$\mu_2 = 2a\alpha\beta - \omega = (2a/L^2)\,\Phi(\ln q) - \omega \qquad \text{or} \tag{11b}$$

$$\mu_2 = \omega[(a_A/a_{true}) - 1]. \tag{11c}$$

Equation (11a) is identical to Eq. (5); note that the true a from Eq. (8) or Eq. (10) must be used here. Equation (11c) is obtained by combining the value of a calculated by Ångström's formula [Eq. (4)], a_A, with the correct value obtained using Eq. (8) (taking μ_2 into account), a_{true}.

2.2. Convection Effects

No theory for the case of radial heat loss by convection in an Ångström experiment has ever been developed. However, heat transfer by convection from long, thin cylinders is technologically important and has been extensively studied. The steady-state heat loss from heated wires or cylinders can be accurately calculated [11, 12] and some information is available on heat loss from periodically heated planes [11, 13] and even (thick) cylinders [11, 14]. The steady-state heat loss from rods with various axial temperature distributions has also been studied [11, 15]. However, in the present case we need to know the heat loss per unit surface area from a thin rod, heated periodically at one end, and with an exponential longitudinal temperature distribution. This case has never been studied theoretically, and we do not attempt to develop such a theory. Instead we use the available information about periodic heat loss from thick cylinders [11, 14] and planes [11, 13] to find some general guiding principles.

At low frequencies the convection currents follow the variations in T, but with some time delay τ. If ω is very low it is reasonable to assume that τ is constant and independent of ω, corresponding to a phase shift $\tau\omega$ radians. In this case

$$\mu_2 = \mu_1 \tan \tau\omega \simeq \mu_1 \tau\omega \tag{12}$$

Neither of the methods presented above can now be used to measure a, but an exact expression can still be found for a as a function of α and β:

$$a = \omega_1\omega_2(1 - Q_1)/(\omega_2\alpha_1\beta_1 - \omega_1\alpha_2\beta_2) \tag{13}$$

The practical usefulness of Eq. (13) is doubtful, since it is valid only in the limit $\omega \to 0$, with a corresponding large uncertainty in Φ and q; also, at low ω, $\mu_1 \simeq$ constant and thus $Q_1 \simeq 1$, which also decreases the experimental accuracy. In analogy with Eq. (8) we can also write

$$a = (\omega + \mu_2)/2\alpha\beta = (\omega/2\alpha\beta)(1 + \tau\mu_1) = a_A(1 + \tau\mu_1) \tag{14}$$

Since τ must be negative, the measured a is always smaller than the true a. At very high frequencies the convection currents are constant, and the heat loss is the sum of a constant convective term and a variable conduction

term of the form of Eq. (6). We assume that the constant term affects only the mean longitudinal temperature distribution in the rod. The heat loss seen by the temperature wave is then only that due to radial conduction from the rod, and the theory for the two-frequency method [4] should apply.

Between these two extreme situations, we should have a broad transition regime, where no simple theory is valid.

3. EXPERIMENTS

3.1. Experimental Method and Equipment

The present experiments were carried out on a piece of commercial constantan thermocouple wire (for use with Cu; nominal composition, 60% Ni and 40% Cu) with a nominal diameter of 0.812 mm (0.032 in.), obtained from Omega Engineering Co., U.S.A. Constantan was chosen partly because few data are available on its thermal transport properties, and partly because we needed a material with a low thermal diffusivity in order to minimize reflection problems at very low frequencies (see below).

The experimental procedure and the computer-based measurement system used have been described elsewhere [2]. The specimen studied was mounted vertically at the axis of a cylindrical container that could be either evacuated or filled with a suitable fluid. The fluids used are specified in Table I, in which we also give literature data for their thermophysical properties. Chromel wires, 0.15 mm in diameter, were spot welded to the

Table I. Thermophysical Properties at 295 K of the Fluids Used in the Present Investigation[a]

Fluid	λ ($W \cdot K^{-1} \cdot m^{-1}$)	a ($m^2 \cdot s^{-1}$)	ν ($m^2 \cdot s^{-1}$)	α (K^{-1})
Air	0.026 [16]	2.2×10^{-5}[b]	1.6×10^{-5}[c]	3.4×10^{-3}
Hexane	0.12 [17]	8.3×10^{-8}[b]	4.8×10^{-7}[c]	1.4×10^{-3} [22]
Silicone oil[d]	0.12 [18]	8.3×10^{-8} [18]	1.0×10^{-6}[e]	1.3×10^{-3}[e]
Ethylene glycol	0.25 [19]	9.8×10^{-8}[b]	1.6×10^{-5} [19][c]	6.9×10^{-4} [19]
Glycerol	0.29 [20]	9.7×10^{-8} [20]	9.9×10^{-4}[c]	4.0×10^{-4} [22]

[a] λ is the thermal conductivity, a is the thermal diffusivity, ν is the kinematic viscosity, and α is the volume thermal expansion coefficient. Numbers in brackets refer to references.
[b] Calculated from λ, using density data from Ref. 16 and data for c_p from Ref. 21.
[c] Calculated using data for density and/or viscosity from Ref. 16.
[d] Dow Corning DC200 fluid.
[e] Manufacturer's data.

specimen at the cold end and at the two measurement points, such that the sample itself was used as one leg of a differential thermocouple for the measurements [2, 4]. Two Alumel wires of the same diameter were also welded to the specimen, at the cold end and at the first (upper) measurement point, respectively, in order to find the actual temperature of the specimen [2].

3.2. Experimental Results

Figure 1 shows the results obtained for the thermal diffusivity a of the specimen at 300 K, when immersed in various fluid media. a was calculated from the experimental data for q and Φ using Ångström's original method [Eq. (4) above]. We have plotted a versus the period $\Omega = 2\pi/\omega$, which was normally varied between 1 and 1000 s in logarithmic steps (1–2–5 sequence). Since the mean temperature T between the measurement points was kept constant at 300 (± 2) K irrespective of the medium or of the frequency used, the temperature signal varied significantly, with wave amplitudes of >5 K at low ω, decreasing continuously toward zero at high ω, with a corresponding inverse variation in the precision of the measurements of a. At very low ω the precision was also low, since Φ and

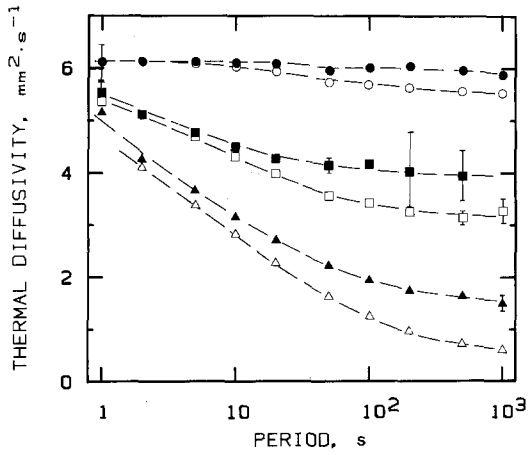

Fig. 1. Thermal diffusivity, a, for constantan, calculated from experimental data using Eq. (4), versus the period of the temperature wave. Dashed lines are guides for the eye only. Symbols denote the various media surrounding the specimen: ●, specimen in a vacuum; ○, in air; ■, in hexane; □, in silicone oil (DC200 fluid); ▲, in ethylene glycol; △, in glycerol.

$\ln q$ both approached zero. Each point in Fig. 1 denotes the mean of between 5 (at high Ω) and 30 (at low Ω) measurements. The standard deviation from the mean was normally smaller than the size of the symbol, but in a few cases larger values were observed (shown by error bars).

Figure 2 shows the corresponding values of q and Φ as functions of Ω from the same experiments. The solid lines show, as a comparison, theoretical values corresponding to the case $\mu = 0$ (or $\mu << \omega$), calculated from Eqs. (3) using the experimental value $a = 6.19 \times 10^{-6}\,\mathrm{m^2 \cdot s^{-1}}$ (see below). The vacuum results follow these curves very closely up to about $\Omega = 30$ s, but we also note that the experimental data for Φ follow the corresponding theoretical curve very well all the way up to $\Omega = 1000$ s even in some liquid media, notably glycerol. This effect results from the structure of Eq. (3b) and was discussed in some detail in Ref. 4 as the basis of the "phase" method of measuring a.

It is obvious from Figs. 1 and 2 that the presence of a fluid medium has a large effect on the measured values of Φ and q, and thus also on a, with the "best" results being obtained at high ω. Note, however, that a depends on ω even in a vacuum. This is due mainly to heat loss through the thermocouple wires: the change in thermal impedance at the welds gives rise to small reflected temperature waves which interfere with the measurements. In Fig. 3 we show the air and vacuum data together with the results (solid line) of a simple calculation of these effects, using the

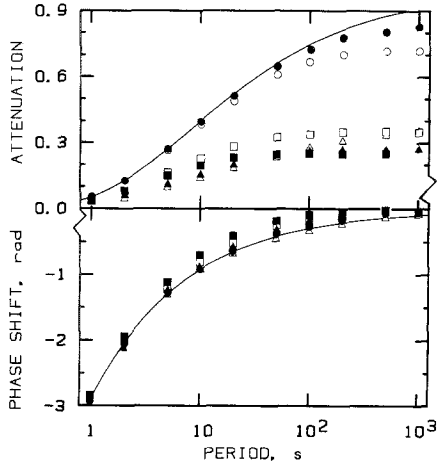

Fig. 2. Attenuation q and phase shift Φ versus period from the same experiments as in Fig. 1. Solid curves are calculated for the case $\mu = 0$. Symbols used are the same as in Fig. 1.

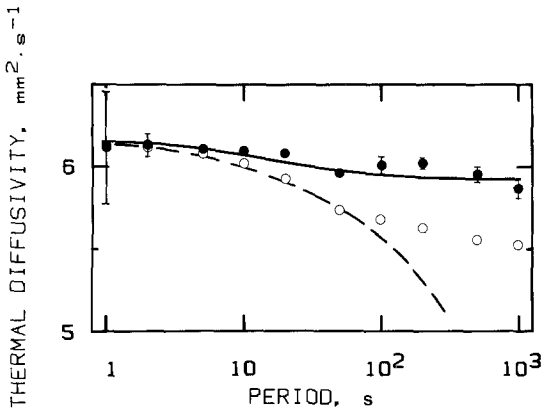

Fig. 3. Thermal diffusivity a versus period with the sample in air and in a vacuum. Solid curve was calculated using the transmission line model and shows the effect of temperature wave reflections; dashed curve was calculated using the same model but also taking into account the effect of the imaginary heat loss coefficient μ_2, as calculated for still air. Symbols are the same as in Fig. 1.

transmission line model [23] and a value for a of $6.185 \times 10^{-6}\,\mathrm{m^2 \cdot s^{-1}}$. It is clear that most of the deviations from linearity in the vacuum experiment are due to this effect. The small extra deviations at high Ω are probably due to the decrease in attenuation: since $q \to 1$ as $\Omega \to \infty$, a small temperature wave will reach the thermocouple at the cold end at sufficiently high Ω. Since the temperature is measured differentially between this thermocouple and those at the measurement points, this will result in an experimental error. From the dimensions of the specimen, we calculate that a residual wave with an amplitude 0.1 % of that at the first measurement point will appear at the cold end at $q = 0.61$, increasing rapidly to 1 % at $q = 0.72$. In a vacuum, these values correspond to $\Omega \simeq 30$ and 100 s, respectively, in good agreement with the region where deviations from the calculated curve are observed. The calculations also show that reflections should not change much on changing the environment from a vacuum to air. Since much larger deviations from the calculated curve occur in the latter case, we conclude that other mechanisms must dominate in air. This is discussed further in the next section.

From these results we conclude that the thermal diffusivity of constantan at 305 K is $6.19 \times 10^{-6}\,\mathrm{m^2 \cdot s^{-1}}$. Although the statistical uncertainty is below 0.5 %, the total maximum error is about 3 % due to the uncertainty in the thermocouple distance L. Using $c_p = 401\,\mathrm{J \cdot kg^{-1} \cdot K^{-1}}$, extrapolated from

the data of von Eucken and Werth [24], and a density of $9.8 \cdot 10^3\ \mathrm{kg \cdot m^{-3}}$, we find $\lambda = 22.0\ \mathrm{W \cdot m^{-1} \cdot K^{-1}}$, in good agreement with literature data as given in a recent compilation [25].

4. DISCUSSION

4.1. High-Frequency Limit: The Behaviour of μ_2 and a

The main aim of this investigation was to test the assumptions made above regarding the theory of Ångström's method in a fluid environment, and it is convenient to discuss the high- and low-frequency regions separately, starting with the high-frequency end ($\Omega \to 0$). We postulated that for small Ω and large viscosities convection currents were constant and should not influence the measurements. We should then be able to calculate accurately the imaginary heat loss coefficient μ_2 using Eq. (6), provided that the thermal properties of the fluid medium and the specimen are known. We should also be able to use the two-frequency method of Sundqvist and Bäckström [4], Eq. (10), to find accurate values of a from the experimental data for q and Φ.

In Fig. 4, we show experimental data for μ_2, calculated using Eq. (11b) and experimental data for a, q, and Φ, as a function of Ω. We also show (solid curves) the corresponding theoretical values for μ_2, calculated from

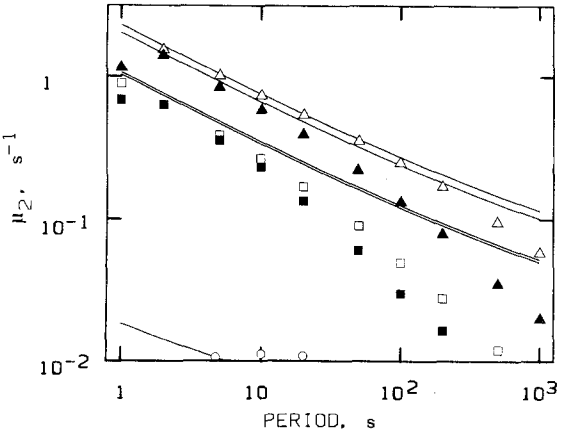

Fig. 4. Imaginary heat loss coefficient μ_2 versus temperature wave period (log–log scales). Solid lines calculated from Eq. (6) using data from Table I; the lines were calculated for (top to bottom) glycerol, ethylene glycol, DC200, hexane, and air (bottom left). Symbols are the same as in Fig. 1 and denote experimental data.

Eq. (6) using data given above and in Table I. The agreement between the two sets of data becomes very good for all fluids below $\Omega = 10$ s, except at $\Omega = 1$ s, where the experimental accuracy is low (see above). As $\Omega \to 0$ we have, approximately, $\mu_2 \sim \Omega^{-1/2}$, and thus $\omega >> \mu_2$ at sufficiently small Ω. From Eq. (8) it follows that the measured value of a should tend toward the true value as $\Omega \to 0$, independently of the surrounding medium, in agreement with the data in Fig. 1. On the other hand, in the high-Ω convection region the experimental slope of μ_2 versus Ω becomes steeper than for the theoretical function, and at high Ω we find $\mu_2 \propto \Omega^{-1}$, in agreement with the prediction in Eq. (12). From Eqs. (4) and (14) this is equivalent to a constant (but too low) experimental value for a, again in agreement with Fig. 1.

In Fig. 5 we show again the same data as in Fig. 1 for fluid media, but now together with theoretical curves for $a(\Omega)$ calculated from the inverse of Eq. (11c) using $a_{\text{true}} = 6.19 \times 10^{-6}\ \text{m}^2 \cdot \text{s}^{-1}$ and the calculated $\mu_2(\Omega)$. The corresponding theoretical curve for air is also shown as a dashed line in Fig. 3. These curves thus show how the experimental values of a should depend on Ω, if Ångström's original method were used and the specimen was encased in a medium with the same thermal properties as the medium actually used, but free from convection. Any differences between these

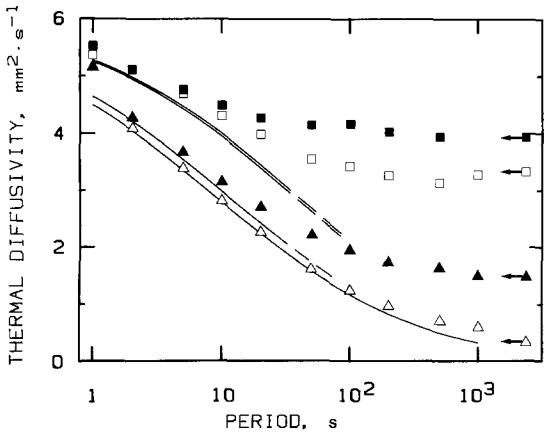

Fig. 5. Same data and symbols as in Fig. 1. Curves show theoretical values for a, as calculated from theoretical data for μ_2. The curves were calculated for (top to bottom) hexane, DC200, ethylene glycol, and glycerol. The calculated curves are not shown at large periods, to avoid data overlap. Arrows with symbols denote the limiting values for a as $\Omega \to \infty$, as calculated from Eq. (14).

curves and the actual experimental data must thus be caused by convection. We observe that the differences are indeed small, provided either that Ω is small or that the medium is highly viscous. Note particularly that even in the case of air (Fig. 3), μ_2 is large enough to cause a significant experimental error at $\Omega > 5$ s, an error rapidly increasing with Ω until limited by convection effects above 50 s. The large magnitude of μ_2 is here due mainly to the small radius of the specimen [Eq. (6)]. Ångström's method is usually recommended for use in air or in inert gas media, but this particular source of error is rarely taken into account in spite of the fact that it can easily dominate the total error for thin samples. On the other hand, we also note that convection to some extent is a benevolent effect, counteracting and limiting the error caused by conduction heat loss.

Finally, we show in Fig. 6 experimental data for a, calculated from the same experimental data for Φ and q as used in Fig. 1, but using the two-frequency method [Eq. (10)]. a is plotted versus the geometric mean Ω_m of the periods used, $\Omega_m = 2\pi/(\omega_1\omega_2)^{1/2}$. The results shown look somewhat similar to those in Figs. 1 and 5, but now the data obtained in the fluid with the highest viscosity, glycerol, are independent of ω at low Ω, in agreement with the discussion above. As expected, the results obtained in all media tend toward a constant value near $6.19 \times 10^{-6}\ \mathrm{m^2 \cdot s^{-1}}$ as $\Omega \to 0$; for some unknown reason, however, the glycerol data are high by about 2%.

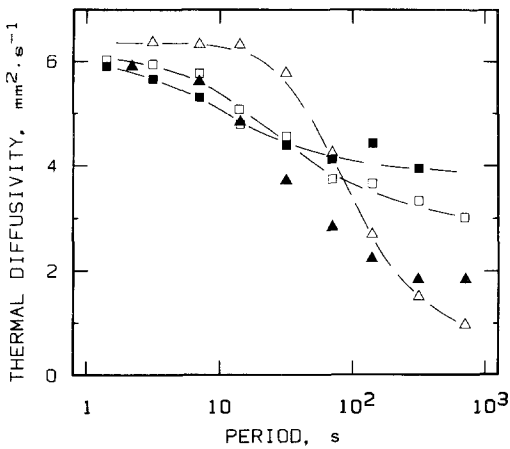

Fig. 6. Thermal diffusivity a versus period, as calculated from the data in Fig. 2 using the two-frequency model, Eq. (10). The results are plotted versus the geometric mean of the periods used. Dashed lines are guides for the eye only. Symbols are the same as in Fig. 1.

4.2. The Low-Frequency Limit: The Behavior of μ_1 and a

In Fig. 7, we show experimental data for the real heat loss coefficient μ_1, as calculated from Eq. (11a) and experimental data for Φ and q, using $a = 6.19 \times 10^{-6}\ \mathrm{m^2 \cdot s^{-1}}$. As a comparison we also show (solid curves) theoretical data for μ_1 for the case of pure conduction, again calculated from Eq. (6) using data from Table I. As for μ_2, the agreement between the two sets of data becomes quite good as $\Omega \to 0$, particularly for glycerol; the experimental data for ethylene glycol and hexane, however, deviate strongly from the theoretical curves at 1 s, probably because of experimental errors (see above). At large Ω convection effects add a large component to μ_1, and no agreement can be expected. However, in the case $\Omega \to \infty$, i.e., constant temperature, we should also be able to calculate μ_1 accurately. For long, horizontal, thin cylinders Morgan [12] gives the relation

$$\mathrm{Nu} = C\,\mathrm{Ra}^m \tag{15}$$

between the Nusselt number Nu and the Rayleigh number Ra; in our notation

$$\mathrm{Nu} = \mu_1 r^2 \rho c_p / \lambda_m \tag{16}$$

$$\mathrm{Ra} = 8 g \alpha_m r^3 T / v a_m \tag{17}$$

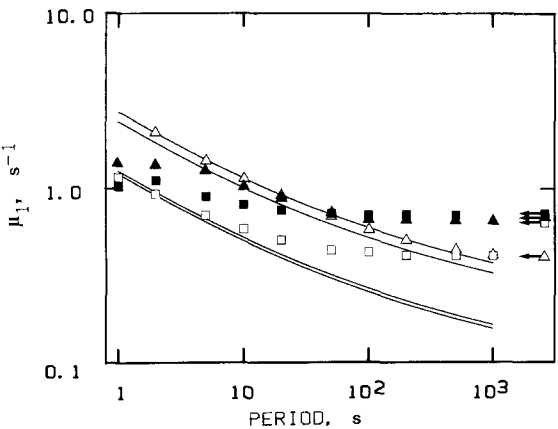

Fig. 7. Real heat loss coefficient μ_1 as a function of period. Curves are calculated from Eq. (6) for (top to bottom) glycerol, ethylene glycol, DC200, and hexane. Symbols are the same as in Fig. 1. Arrows with symbols denote theoretical values for the case of constant natural convection and were calculated using Eq. (15).

Here C ($\simeq 1$) and m ($\simeq 0.2$) depend on Ra, $g = 9.822\ \mathrm{m \cdot s^{-2}}$ in Umeå, α_m is the volume thermal expansion coefficient of the medium, and ν is its kinematic viscosity. For a vertical sample, Morgan suggests that the value of μ_1 given by Eq. (15) should be reduced by a factor of 2. However, Al-Arabi and Khamis [26] have shown that this is true only for infinitely long cylinders and that μ_1 is almost independent of inclination angle for length-to-diameter ratios between 20 and 50, which includes the effective ratio for the warm part of our specimen. We have therefore calculated μ_1 ($\Omega \to \infty$) for our media using Eq. (15) directly, with values of C and m chosen according to Morgan [12]. The results are given in Table II and shown as arrows on the right-hand border of Fig. 7. The agreement between the experimental and the theoretical values is surprisingly good: only for the silicone oil (open squares) is there a significant difference between the two sets of data. We believe that this large discrepancy must be due to some error in the manufacturer's data used (Table I).

As a final test, we have used the data for μ_2 from Fig. 4 to calculate τ. In the low-frequency range we assumed a model in which $\mu_2 = \mu_1 \tau \omega = 2\pi\mu_1 \tau \Omega^{-1}$ [Eq. (12)], and the slope of μ_2 versus Ω thus immediately gives $\tau\mu_1$. We can then either use this to find τ, since the low-frequency value of μ_1 is known, or use $\tau\mu_1$ directly to calculate the limiting low-frequency value of a from Eq. (14), as $a = 6.19 \times 10^{-6}(1 + \tau\mu_1)$. The results for τ are given in Table II, while the results of the latter calculation are shown as arrows on the right-hand border of Fig. 5. For air, the predicted value is $5.52 \times 10^{-6}\ \mathrm{m^2 \cdot s^{-1}}$, which can be compared to the data in Fig. 3. Again, the agreement between the predictions and the experimental data is excellent, except for glycerol, where $\Omega = 1000$ s is not high enough to obtain the limiting value for a in the experiment.

Table II. Experimental and Calculated Values for Some Heat Loss Properties (See Text for Details)

Property	Air	Hexane	DC200	Ethylene glycol	Glycerol
μ_1 ($\Omega \to \infty$)					
Exp.	0.040	0.70	0.41	0.64	0.40
Eq. (13)	0.040	0.70	0.64	0.68	0.40
$-\tau$ (s)	2.8	0.8	2.1	5.0	>40
τ_0					
Exp.	5	<1	<1	<2.5	<25
Eq. (17)	0.1	0.26	0.37	2.0	18

4.3. Transition Frequency

Although the most important aim of this investigation was to confirm the model given above, a secondary goal was to find a criterion for the choice of pressure transmitting medium in a high-pressure experiment. What we need to know is the lowest value required for the viscosity of the pressure transmitting medium, given the thermal transport properties of the medium and the specimen, and the dimensions of the specimen.

The two-frequency method [Eq. (10)] works as long as the convection currents do not change significantly during half a period of the temperature wave. Our first attempt to estimate the time τ_0 necessary for convection currents to change was to use the expression of Parsons and Mulligan [27] for the time at which convection develops around a suddenly heated wire; in our notation

$$\tau_0 = 136(r^2/a_m)(\mathrm{Ra} \cdot \mathrm{Nu})^{-0.58} \tag{18}$$

This expression, however, contains μ_1 [through Nu; see Eq. (16)], which is a complicated function of many parameters, making calculations difficult. Also, the expression was found to overestimate significantly the usable frequency range. We have therefore used instead the expressions given by Siegler [28] for transient convection near a vertical flat plate. For this case, Siegler found that on changing the temperature of the plate, no convection occurred until at a time

$$\tau_0 = 1.80[r(1.5a_m + \nu)/(g\alpha_m a_m \Delta T)]^{1/2} \tag{19}$$

Using, again, data from Table I we have calculated τ_0 from Eq. (19) for the media used, and we present the results in Table II. These data should be compared with one half of the highest value of Ω at which Eq. (10) gives "correct" values for a, and these are also shown in Table II. Unfortunately, it is only for glycerol that we can make a reasonably valid comparison, but in this case the agreement is very good, and using $\Omega_{max} = 2\tau_0$ from Eq. (19) is, at present, the best available criterion for choosing a "convection-free" pressure medium. For air, theory predicts $\tau_0 = 1$ s, but no significant deviations from the "conduction corrected" values of a occur until at > 50 s (see Fig. 3). This, however, is not surprising, since $\mu_2 << \omega$ at low Ω, and neither convection nor conduction heat loss should have a large effect until μ_2 is a significant fraction of ω. Equation (19) is thus useful mainly for prediction of the convection limit of dense fluids.

5. CONCLUSIONS

From the discussion above, we conclude that the simple model assumed above gives a very good quantitative description of convection heat loss in an

Ångström-type experiment, both at low and at high frequencies. Although no exact theory has been found for the intermediate-frequency range, this is of little importance here, since we are really interested only in the high-frequency range, where the Sundqvist–Bäckström two-frequency method [4] is valid. We have found that it is possible to calculate accurately both the magnitude and the relative phase of the heat loss at high frequencies. It is thus possible to measure approximate values of a in this range using Ångström's method and then to use theoretical values of μ_2 to calculate the true values. Conversely, at low frequencies (large Ω) we can calculate only the real part of the heat loss, but by measuring a and the heat loss as functions of Ω it is again possible to deduce correct values for a using the ratio of real-to-imaginary heat loss coefficients. Alternatively, measurements in this frequency range can be carried out using a new variety of Ångström's method presented here as Eq. (13) and valid only under conditions of heavy convection heat loss. We have also shown that, even in air, conduction and convection heat loss can cause large experimental errors for thin specimens, and finally, we have found a fairly simple criterion for choosing a suitable fluid high-pressure medium in which high-accuracy thermal diffusivity measurements by the two-frequency method are possible.

ACKNOWLEDGMENTS

I would line to thank my collegues Dr. Per Jacobsson (now at Chalmer's University, Gothenburg, Sweden) and Dr. Staffan Andersson (now at the Department of Applied Physics, Umeå University) for useful discussions at various stages of this work.

REFERENCES

1. B. Sundqvist, *Mat. Res. Soc. Symp. Proc.* **22** Pt. I:261 (1984); R. G. Ross, P. Andersson, B. Sundqvist, and G. Bäckström, *Rep. Prog. Phys.* **47**:1347 (1984); P. Jacobsson and B. Sundqvist, *Phys. Rev. B* **40**:9541 (1989).
2. P. Jacobsson and B. Sundqvist, *J. Phys. Chem. Solids* **49**:441 (1988).
3. P. Jacobsson and B. Sundqvist, *Int. J. Thermophys.* **9**:577 (1988).
4. B. Sundqvist and G. Bäckström, *Rev. Sci. Instrum.* **47**:177 (1976).
5. A. J. Ångström, *Ann. Phys. Chem.* **64**:33 (1861).
6. G. C. Danielson and P. H. Sidles, in *Thermal Conductivity, Vol. 2*, R. P. Tye, ed. (Academic, London, 1969), p. 154.
7. L. P. Phylippov, in *Compendium of Thermophysical Property Measurement Methods, Vol. 1*, K. D. Maglić, A. Cezairliyan, and V. E. Peletsky, eds. (Plenum, New York, 1984), p. 337.
8. B. Sundqvist, *Rev. Sci. Instrum.* **52**:1061 (1981).
9. J. E. Parrot and A. D. Stuckes, *Thermal Conductivity of Solids* (Pion Press, London, 1975), p. 24; L. Verdini and A. Santucci, *Nuovo Cim.* **62B**:399 (1981).

10. H. S. Carslaw and J. C. Jaeger, *Conduction of Heat in Solids*, 2nd ed. (Clarendon, Oxford, 1959).
11. A. J. Ede, *Adv. Heat Transf.* **4**:1 (1967), and references therein.
12. V. T. Morgan, *Adv. Heat Transf.* **11**:199 (1975).
13. P. Singh, V. P. Sharma, and U. N. Misra, *Ind. J. Pure Appl. Math.* **9**:182 (1978); R. S. Rath and G. Jena, *Int. J. Heat Mass Transf.* **23**:1598 (1980).
14. J. H. Merkin, *J. Fluid Mech.* **30**:561 (1967); R. S. Nanda and P. K. Muhuri, *Proc. Ind. Natl. Sci. Acad. A* **43**:385 (1977).
15. H. R. Nagendra, M. A. Tirunarayanan, and A. Ramachandran, *Nucl. Eng. Design* **16**:153 (1970), **16**:163 (1970); V. N. Pustovalov and Yu. Ya. Matveev, *J. Eng. Phys.* **43**:853 (1982).
16. R. C. Weast, *CRC Handbook of Chemistry and Physics*, 60th ed. (CRC, Cleveland, 1979).
17. Y. Tanaka, Y. Itani, H. Kubota, and T. Makita, *Int. J. Thermophys.* **9**:331 (1988).
18. O. Sandberg and B. Sundqvist, *J. Appl. Phys.* **53**:8751 (1982).
19. D. Bohne, S. Fischer, and E. Obermeier, *Ber. Bunsenges. Phys. Chem.* **88**:739 (1984).
20. O. Sandberg, P. Andersson, and G. Bäckström, *J. Phys. E* **10**:474 (1977).
21. Y. S. Touloukian and T. Makita, *Thermophysical Properties of Matter, Vol. 6. Specific Heat—Nonmetallic Liquids and Gases* (IFI/Plenum, New York, 1970).
22. N. B. Vargaftik, *Tables on the Thermophysical Properties of Liquids and Gases* (Hemisphere, Washington, D.C., 1975).
23. D. H. Howling, E. Mendoza, and J. E. Zimmerman, *Proc. Roy. Soc.* **229**:86 (1955); R. Horch, *Exp. Techn. Phys.* **23**:97 (1975).
24. A. von Eucken and H. Werth, *Z. Anorg. Allgem. Chem.* **188**:152 (1930).
25. C. Y. Ho, M. W. Ackerman, K. Y. Wu, S. G. Oh, and T. N. Havill, *J. Phys. Chem. Ref. Data* **7**:959 (1978).
26. M. Al-Arabi and M. Khamis, *Int. J. Heat Mass Transf.* **25**:3 (1982).
27. J. R. Parsons, Jr., and J. C. Mulligan, *Rev. Sci. Instrum.* **49**:1460 (1978); *Trans. ASME* **102**:636 (1980).
28. R. Siegel, *Trans. ASME* **80**:347 (1958).